Section 1
LASER SYSTEM REPORT

1.A GDL Facility Report

The GDL facility continued operations during the second quarter of FY82 in support of the 3ω interaction program, the National Laser Users Facility (NLUF), and the Damage Testing Facility (DTF).

A total of 688 shots were delivered by the facility in the period January 1 to March 31, 1982. The shot distribution was as follows:

3ω Target Experiments	225	Shots
NLUF	141	
DTF	229	
Alignment and Calibration	93	
TOTAL	688	Shots

National Laser Users Facility operations during this time included shots for users from the University of Maryland, UCLA, Yale, NRL, and for the x-ray biophysics group.

1.B OMEGA Facility Report

During the quarter January 1 to March 31, 1982, 432 OMEGA system shots were fired. The principal activity on the system was experimental target shooting. In fact, both the absolute number and the percentage of target shots set new quarterly records.

To accomplish the projected target shot schedule, the Laser Operations Group concentrated on maintaining and firing OMEGA. No significant modifications were attempted and no major failures occurred. On the two scheduled shooting days per week, staggered shift assignments allowed 14–16 hour shooting stints—an effective way to boost the shot rate.

Table 1 is the breakdown by category of the system shots for this quarter. Figure 1 is the shot energy histogram for all the 24-beam shots. The lower energy shots were mostly prescribed in advance. Only 3 of the shots represent system misfires. During the entire period the new 3-meter oscillator was configured for 1 nsec pulses. For all target shots the mean and standard deviation for the pulse duration was 0.963 nsec ± 0.143 nsec.

Beam balance, the ratio of rms fluctuations to mean energy, was 9.3% ± 4.2% for all target shots except those with deliberately unbalanced beam energies.

Table 1
OMEGA laser system shot category distribution January 1 to March 31, 1982.

January 1, 1982 - March 31, 1982

CATEGORY	NUMBER OF SHOTS	PERCENT
Target Shots	193	45
Driver Align and Test	122	28
Beamline c/o and Calibration	49	11
Software Test and Timing	52	12
Miscellaneous, Other	16	4
TOTAL	432	100

G1140

Fig. 1
24-Beam target shots from January 1 to March 31, 1982.

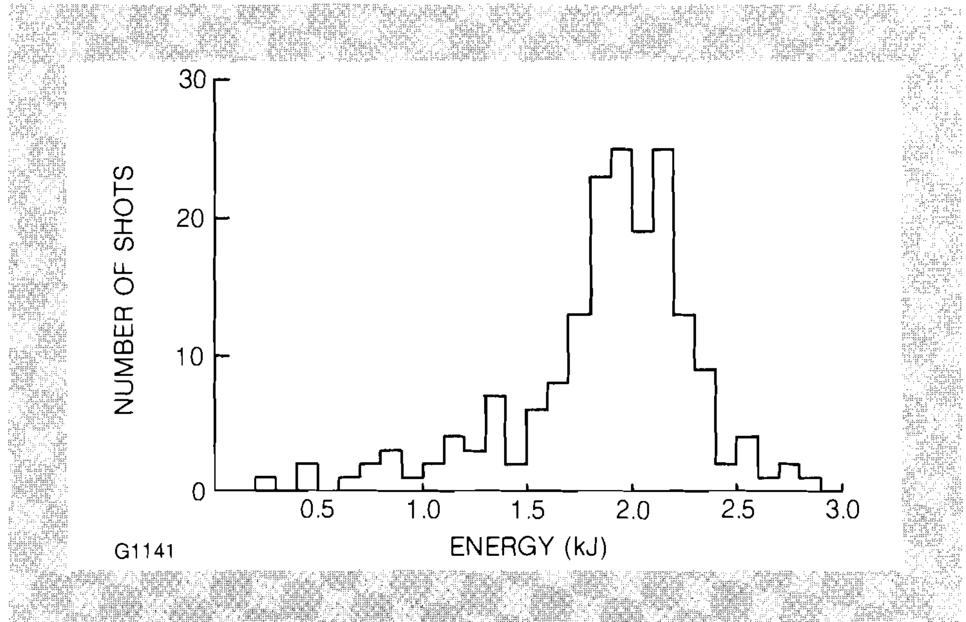

1.C Anisotropic Stress around Defects in Thin Films

Research at LLE is presently being conducted on laser-induced damage in multilayer dieletric thin film coatings. Through the use of optical microanalytical techniques we hope to eventually understand the nature of coating defects which lower the damage thresholds of thin films. Our laser damage tester was described in LLE Review Volume 7, and the use of photoacoustic absorption spectroscopy for defect characterization was discussed in Volume 9. In this issue we describe a second technique for looking at defects in thin films, which is sensitive only to mechanical stress.

Scientific papers[1,2] suggest that there is a correlation between mechanical stress in dielectric multilayer thin films and their laser damage resistance. Work done prior to 1980, however, attempted to investigate the relationship between coating stress and laser damage either indirectly, with calculations based on tabulated data for individual evaporants,[1] or through the use of *spatially averaged* measurements of stress on coated parts with high diameter to thickness aspect ratios.[2] In 1980, T. Lichtenstein proposed and demonstrated[3] that mechanical stress in thin films could be measured using modulated ellipsometry in transmission. Lichtenstein's technique did not require any special coating or substrate geometry and, more importantly, was capable of generating a one-dimensional scan of mechanical stress across a coated substrate with *spatial resolution* approaching 10 μm.

With instrument modifications we have refined Lichtenstein's technique. Figure 2 shows our modified apparatus. Mechanical stress is

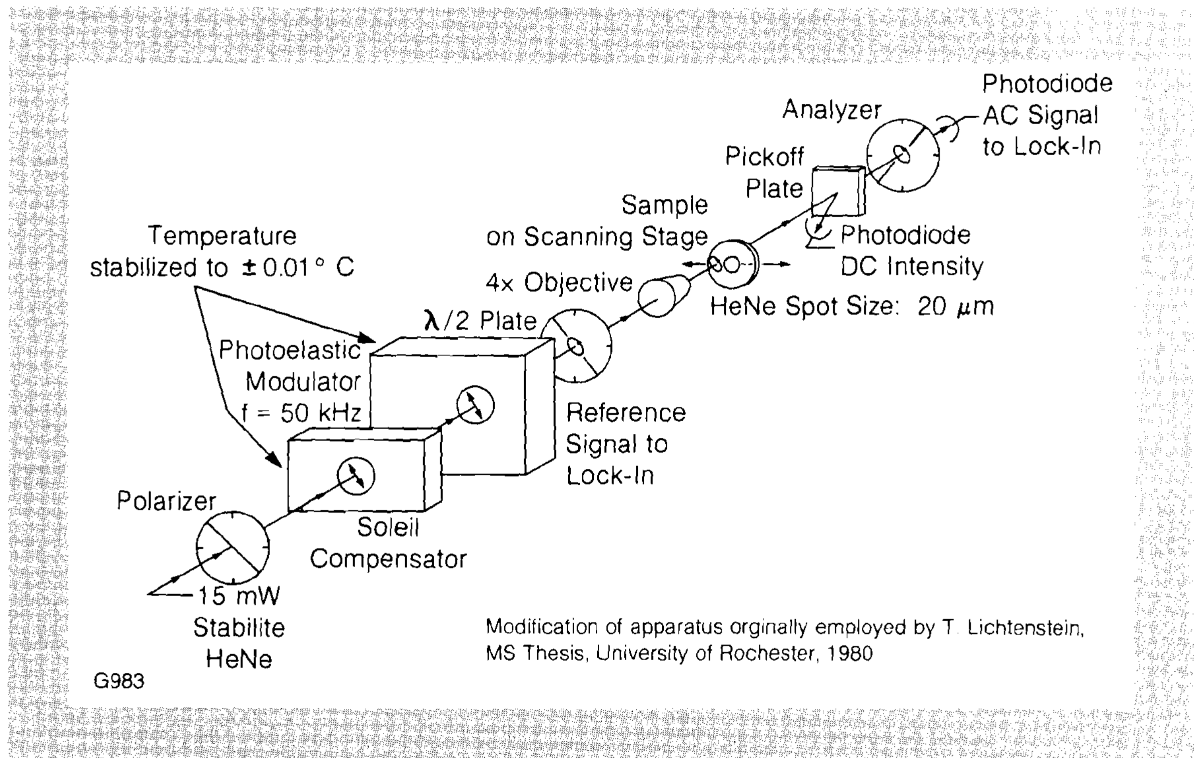

Fig. 2
Apparatus for modulated transmission ellipsometry. Optical retardation in a sample is measured with an ac lock-in amplification technique, using a photoelastic modulator (Hinds International, Inc., model PEM-FS4) operating at a frequency of 50 kHz. Optical retardance is directly proportional to stress in the sample.

wavelength-independent. We therefore use a stable helium-neon laser as our probe source. A photoelastic modulator, (PEM), operating at a frequency of 50 kHz imparts a sinusoidally varying optical phase retardation of $\pm$ 158 nm ($\pm$ $\lambda/4$ at a wavelength of 632.8 nm) to the linearly polarized output of the HeNe. An analyzer converts this phase information to ac intensity and the signal is picked up by a photodiode and displayed on a lock-in amplifier. The lock-in is operated in its high dynamic range mode using an electronic signal from the PEM for reference. A 4X microscope objective focuses the laser beam to a 20 μm spot at the sample plane. Samples are moved transverse to the beam in the focal plane of the objective, at a linear scanning rate of 1 mm/minute. A rotatable half waveplate is incorporated into the apparatus to enable the plane of polarization of the HeNe at the sample to be rotated to any arbitrary orientation with respect to the same translation direction. The analyzer is similarly capable of rotation so that it can always be oriented with its pass direction orthogonal to the polarization direction of light incident on the sample.

The apparatus of Fig. 2 measures the optical phase retardation, Γ, introduced to the laser beam by a sample under investigation. Γ is related to the thickness, t, of the sample and optical anistropy or birefringence, Δn, in the sample as

$$\Gamma(\mathrm{nm}) = t\Delta n \tag{1}$$

The optical phase retardation is directly proportional to the stress, σ, within the sample and can be calculated with a knowledge of sample stress-optic coefficient, c_o, as

$$\sigma(\mathrm{kg/cm^2}) = \Gamma(\mathrm{nm})/c_o\,(\mathrm{nm-cm/kg})\;t\,(\mathrm{cm}) \tag{2}$$

The advantage of measuring stress with modulated transmission ellipsometry is the simplicity of acquiring retardance data. Absolute values of Γ can be obtained provided the apparatus is first calibrated with a Soleil compensator (see Fig. 2). In addition, the sensitivity of the measurement is very high, because it is an ac phase-sensitive technique and because the Soleil compensator can be adjusted to cancel residual birefringence due to all components, other than the sample itself, located between the polarizer and analyzer. Retardance values of 0.01 nm can be measured with excellent repeatability, provided that the Soleil compensator and PEM are temperature stabilized to $\pm 0.1\,^{\circ}$C or better. For a sample 1 μm in thickness, $\Gamma = 0.01$ nm corresponds to an index change of $\Delta n = 0.00001$ and a stress of $\sigma = 50$ kg/cm^2 ($c_o = 2$ nm $-$ cm/kg). Stresses in thin films extend from $\pm$ 3000 kg/cm^2 down, and therefore fall easily within the sensitivity capability of the apparatus.

In addition to high sensitivity, modulated transmission ellipsometry can yield spatially resolved retardance (and therefore stress) information with resolution of 20μm or less. The directionality of stress in samples can also be elucidated by manipulating the polarization direction of the probe laser. The one disadvantage to the technique is a lack of discrimination in the longitudinal direction through the sample being

probed. Stress from both the coating and the underlying substrate add together, and only the algebraic sum is measured. Differentiation between coating and substrate stress is sometimes difficult, and will be examined for a number of examples below.

Modulated transmission ellipsometry of thin films works best when the substrate possesses very little residual internal stress. Figure 3 shows the optical retardance commonly observed in 50 mm diameter by 6.35 mm thick BK-7, fused silica, and "Pyrex" substrates used in this work. Because it is a well-annealed optical glass product, BK-7 exhibits a very small amount of residual internal stress, and therefore constitutes an ideal substrate material. Fused silica, when cut into discs from rod stock, exhibits the radially symmetric retardance profile characteristic of annealed rods. The retardance across the part is still smoothly varying, and quite suitable for stress studies. Possibly because of the presence of index inhomogeneities or striae, "Pyrex" exhibits a very irregular or "noisy" retardance profile, making it a less desirable substrate for investigations of stress in thin film coatings.

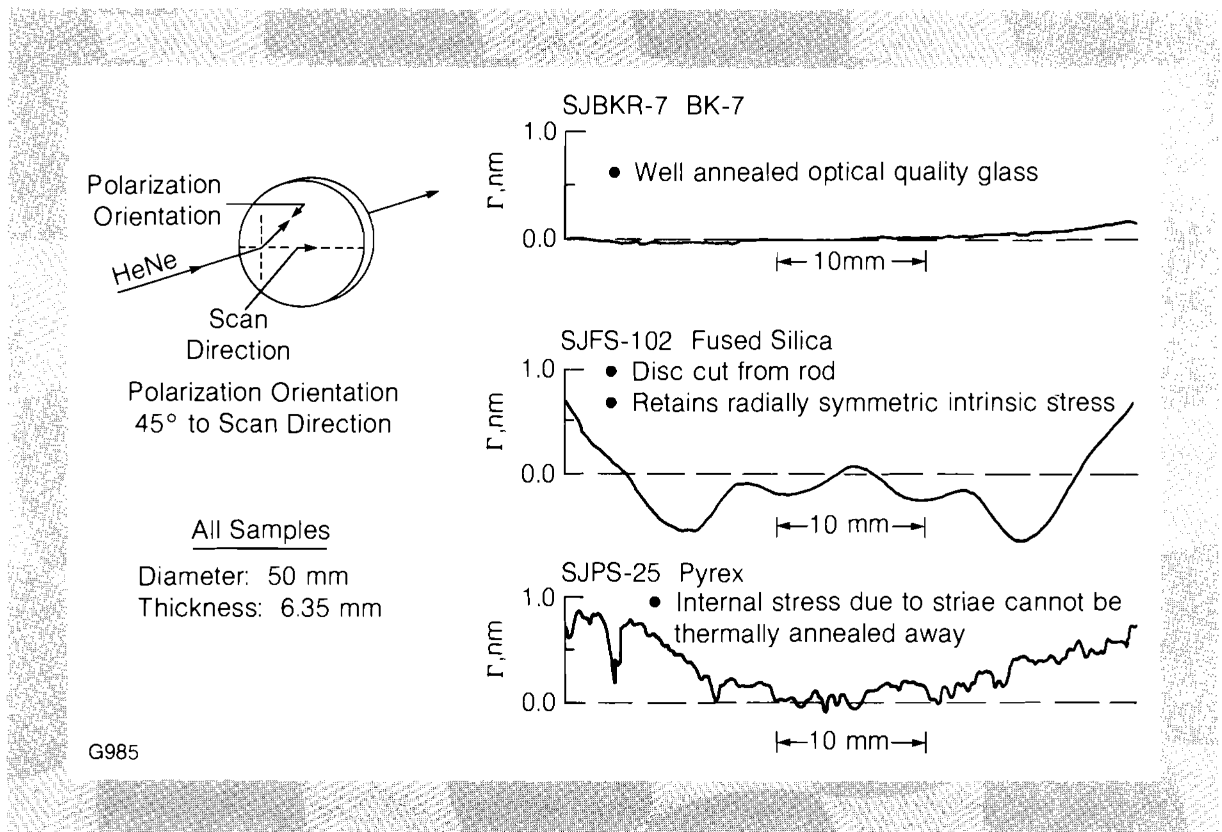

Fig. 3
Residual stress in standard thin film coating substrate materials. BK-7 and fused silica exhibit smoothly varying stress. The stress in "Pyrex" glass shows significant fine structure, making it less desirable as a coating substrate for modulated transmission ellipsometry.

Figure 4 gives the history of the evolution of stress in a coating substrate combination. Figure 4a shows the stress signature of a BK-7 substrate prior to coating. After e-gun evaporation of a $Ta_2O_5 - SiO_2$ multilayer thin film onto the substrate in vacuum at an elevated temperature of 200 °C, the sample exhibits the stress profile indicated in Fig. 4b. Only the central 12 mm diameter portion of the substrate has been coated, in order to show the change in stress across the diameter of the part in transition from uncoated to coated regions. Figure 4c shows the stress

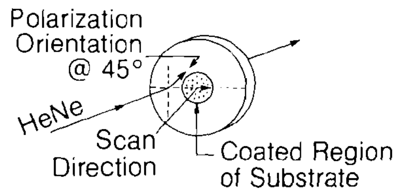

- Substrate: 50 mm diameter × 6.35 mm thick BK-7
- Coating: $HR_{45°}$ @ 351 nm and 1054 nm
- Materials: Ta_2O_5 and SiO_2
- Design: BK-7] $(3H3L)^4$ $3H(LH)^6$ 2L
- Plotted data has been smoothed

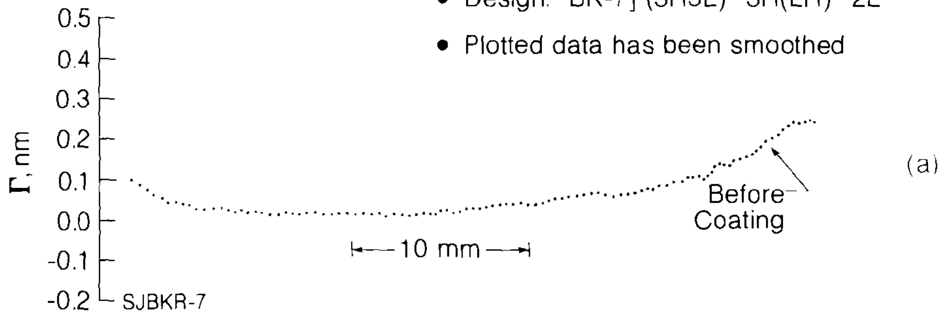

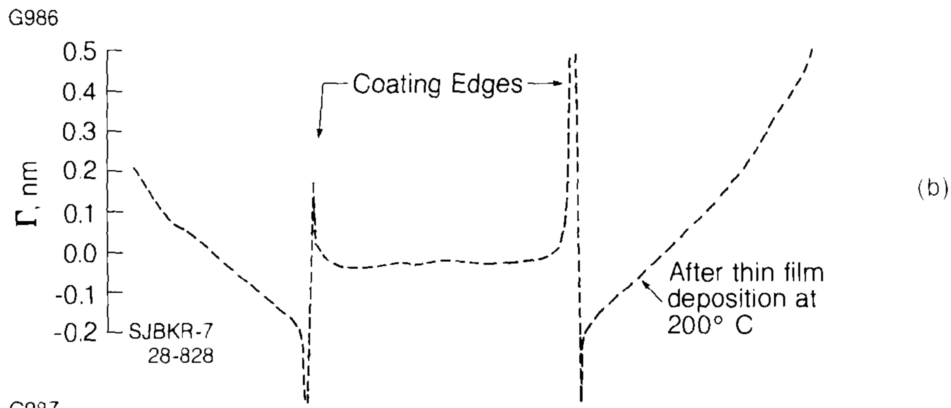

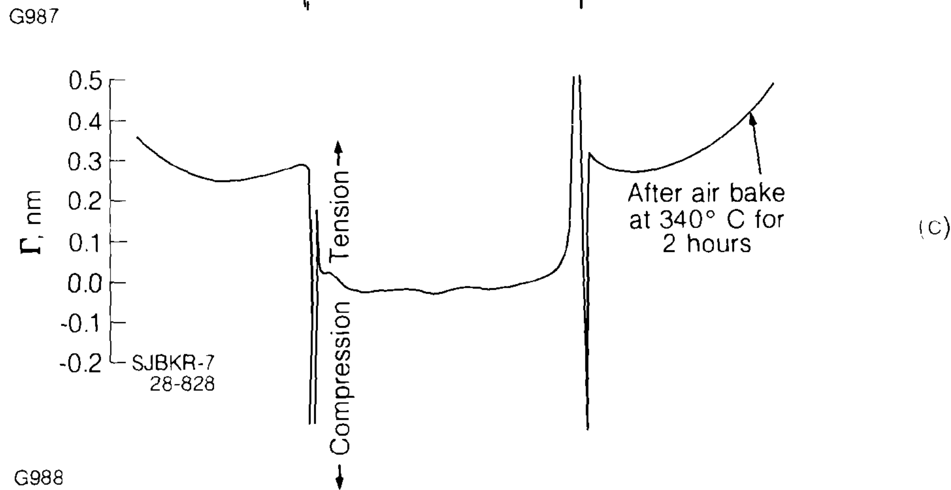

Fig. 4
Evolution of stress in a coating-substrate combination. The sign of stress within the coated region (tensile or compressive) can be inferred from the stress signature of the adjacent uncoated substrate.
a) Optical retardance across substrate prior to coating.
b) Stress induced in substrate after coating deposition at 200°C and exposure to room temperature and humidity.
c) Sign reversal of stress in substrate caused by densification of coating during bake-out at 340°C.
Calibration of optical retardance in terms of tensile or compressive stress was done by measuring the sign of tensile stress in a TiO_2 ditch coating, after Lichtenstein[3] and Heitmann.[4]

profile in this sample after an air bake at 340°C for two hours. Baking of oxide thin films is a standard processing procedure followed at many coating facilities. It helps to complete the oxidation of the evaporants, returning them to their proper stoichiometry. Baking also compacts and densifies the coating layers, driving out water vapor that is chemisorbed upon exposure of freshly coated samples to room temperature and humidity. A comparison of Figs. 4b and 4c shows that there is a reversal of sign to the stress in the BK-7 substrate adjacent to the coated region upon baking. We attribute this sign reversal to the densification process within the coating, in analogy with similar reversals observed by Heitmann for pure SiO_2 films.[4]

A preliminary explanation for the observed profiles is as follows: after deposition and exposure to ambient conditions the coating is in tension. Because it is too thick to deform and relieve the stress created at the coated surface, the uncoated substrate surface goes into compression in regions immediately adjacent to the coating. The sign of stress in the coating changes from tension to compression upon densification during air bake, and therefore the stress in the uncoated substrate adjacent to the coating changes sign to compensate.

There is one observation that does not fit in with the above explanation, and that is the lack of observable stress within the coated region itself. Perhaps the stress present at the coating surface is compensated for in the underlying substrate, and our measurement technique detects the net stress (being equal to zero) for the coating-substrate system. This compensation through the depth of the sample would not occur in uncoated areas where we see indirectly the stress in the coating from its effect on the uncoated adjacent surface.

Modulated transmission ellipsometry measures that component of stress within a sample which lies in a plane perpendicular to the probe beam propagation direction. In this work samples are oriented nearly normal to the probe beam, and the measurement is therefore sensitive to stress in the plane of the thin film coating. Figure 5 shows a retardance scan across a fused silica substrate which possesses a crazed or cracked coating. The stresses generated in the coating during air baking were either larger than the adhesion strength of the coating to the substrate, or exceeded the strength of the coating material itself. Crazing has relieved stress in localized regions of the coating surface, and we can determine the directionality of that stress which remains by varying the polarization of the probe laser. Figure 6 gives high-sensitivity, high-resolution scans across a central area of the coating from Fig. 5, taken with the HeNe probe laser polarized at 45° to the scanning direction (the same as that used in Fig. 5), and with the polarization parallel to the scanning direction. Both scans were generated along the same path across the coating. A photograph of the examined area is reproduced to the same horizontal scale immediately above the retardance scans.

Vertical craze lines 1 and 4 are *not* observed in the lower scan of Fig. 6, because the polarization orientation of the probe beam is parallel to the direction of stress relief immediately adjacent to these features. Op-

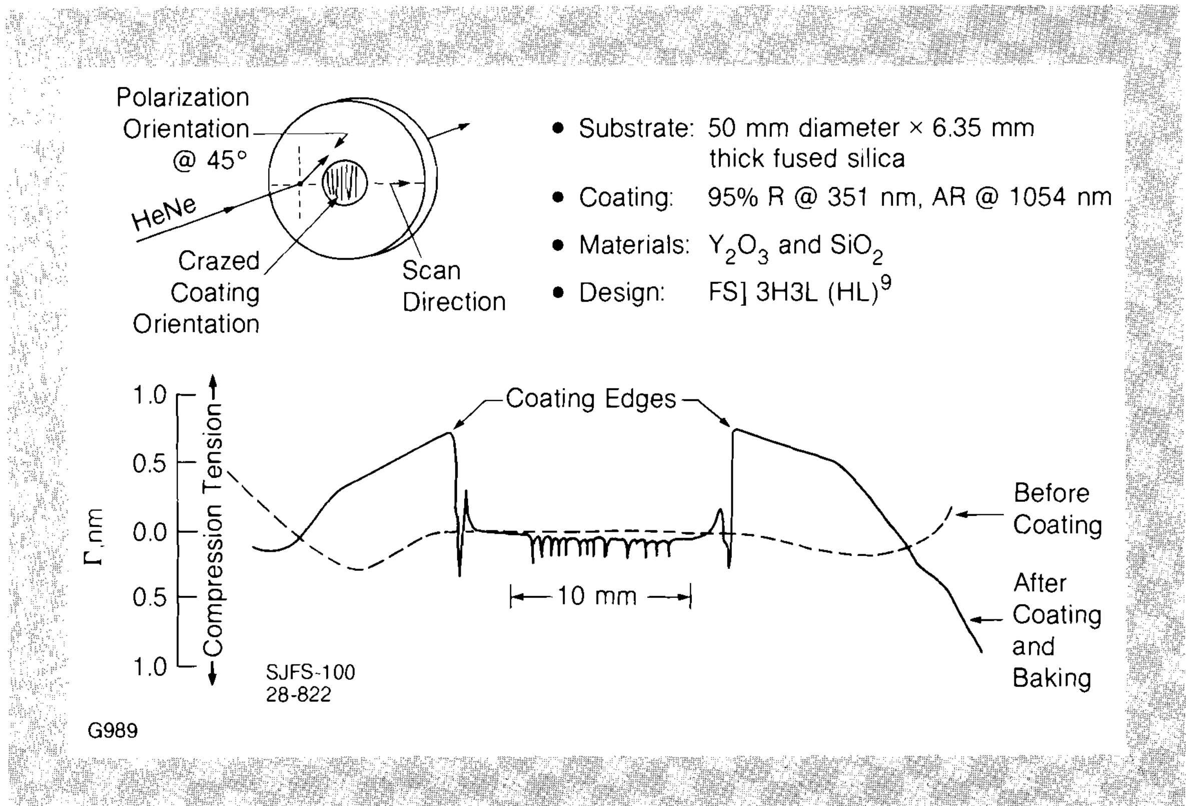

Fig. 5
Anisotropic stress in a crazed coating. A scan across the predominantly vertical craze marks with the probe beam polarized at 45° to the scan direction reveals that stress relief has occurred predominantly in a horizontal direction.

tical retardation can only occur if the probe laser polarization orientation is at some angle other than 0° or 90° to the coating stress. For this reason, the stresses associated with craze lines 2 and 3 are not easily observed with retardance measurements when the probe laser is polarized at 45° to the scanning direction.

Anisotropic stresses associated with absorbing defects in coatings can be mapped out using our modulated transmission ellipsometric technique, provided that the phase-sensitive signal is ratioed to the dc intensity emerging from the sample through the use of a pickoff plate as shown in Fig. 2. In the ratio mode of operation, the apparatus yields retardance data correct to within 10% of the actual coating retardance for defects which attenuate probe beam dc transmittance up to 40%. Figure 7 gives a two-dimensional representation of the compressive and tensile stresses associated with TiO_2 spatter sites embedded in a multilayer TiO_2-SiO_2 high reflectance coating. The data has been plotted in 6 μm by 6 μm grids using a color code and shading scheme given in the legend adjacent to the plot. The stress patterns resemble the Nomarski microphotograph displayed above the 2-D plot, however, the stress does appear to extend over a larger area than that revealed by the photograph. There is a sudden change in film stress from tension to compression at the two defects in the figure and in the region between them. This feature is not detectable through standard optical microscopy.

No laser-induced damage tests have been conducted on absorbing defects for which an anisotropic stress map exists. It has been suggested[1] that, in such a test, regions initially in tension would exhibit a

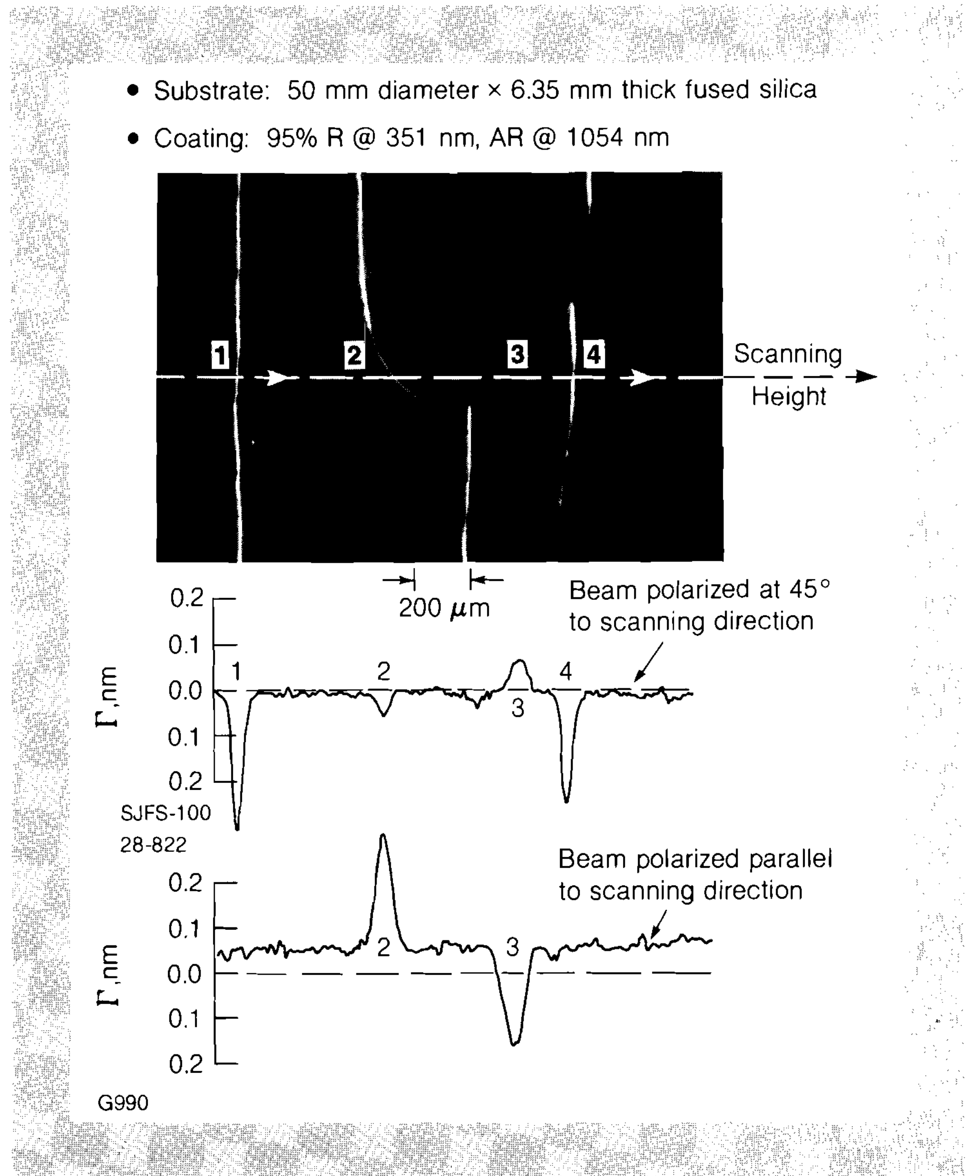

Fig. 6
Polarization sensitivity to stress in a crazed coating. High sensitivity scans across a central region of the coating from Fig. 5 show that the anisotropic stress associated with each craze mark is detectable when the probe beam polarization orientation is at some angle other than 0° or 90° to the cracks.

a) Beam polarized at 45° to scanning direction—stress observable for craze marks 1 and 4.

b) Beam polarized parallel to scanning direction—stress observable for craze marks 2 and 3.

The microphotograph is reproduced to the same horizontal scale as the retardance scans.

higher degree of damage resistance than those initially in compression, due to heat deposited in the absorbing defect and the resultant thermal expansion of the defect and adjacent coating material. In future work we intend to improve the resolution of our modulated transmission ellipsometer apparatus, map anisotropic stress associated with micron size absorbing defects, and correlate the magnitude and sign of anisotropic stress with laser-induced damage. An understanding of the relationship between anisotropic stress around defects and laser damage may enable us to improve the quality of our thin film coatings.

REFERENCES

1. A. Bloom and V. Costich, *NBS Publication 435: Laser-Induced Damage to Optical Materials*, 248 (1975).

2. R. Austin, R. Michaud, A. Guenther, and J. Putman, *Appl. Opt.* **12**, 665 (1973).

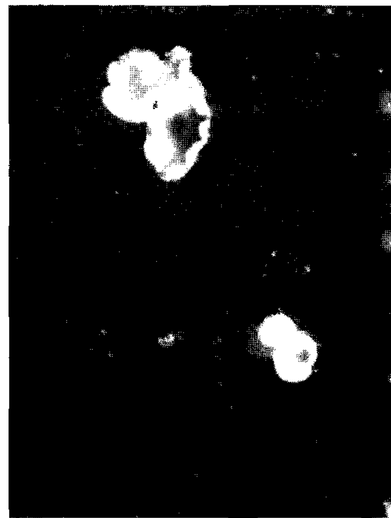

- Coating: TiO_2/SiO_2 multilayer 1.05 μm HR design
- Substrate: 50 mm diameter × 1.6 mm thick plate glass
- Polarization orientation @ +45° to scan direction
- Data acquisition in ratio mode

→| 25 μm |←

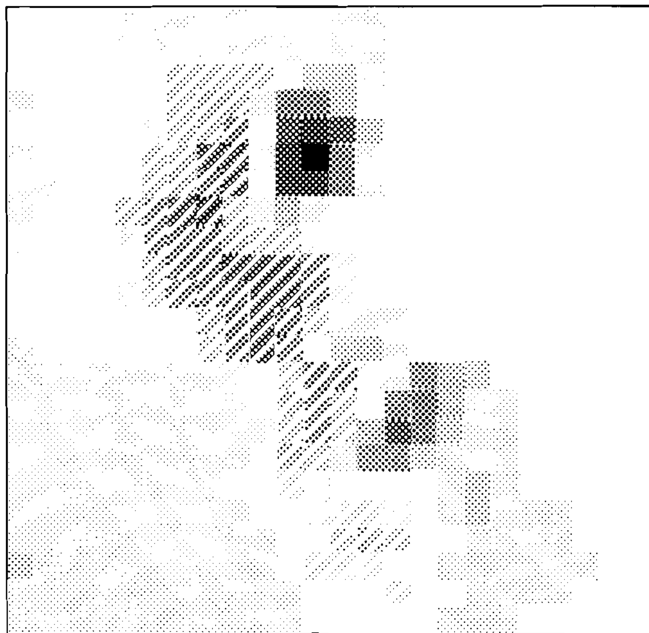

Legend:

Γ,nm	COMPRESSION	TENSION
0.50-0.55		
0.40-0.49		
0.30-0.39		
0.25-0.29		
0.20-0.24		
0.15-0.19		
0.10-0.14		
0.05-0.09		
0.00-0.05		

G991

Fig. 7
Anisotropic stress around absorbing defects. The tensile and compressive nature of stress around two TiO_2 spatter sites in a multilayer dielectric thin film can be compared to a Nomarski microphotograph of the same region.

3. T. Lichtenstein, MS Thesis, Institute of Optics, University of Rochester, 1980.
4. W. Heitmann, *Appl. Opt.* **10**, 2685 (1971).